

A multisource approach for coastal mapping purposes: Limeni bay, Mani and surrounding area, southern Greece

Nikolaos Sabatakakis¹ · Konstantinos G. Nikolakopoulos¹ · George Papatheodorou¹ · George Kelasidis¹

Received: 28 May 2015 / Accepted: 4 January 2016 / Published online: 11 January 2016
© Springer-Verlag Berlin Heidelberg 2016

Abstract A multipurpose engineering geological map of a natural heritage site including inland and offshore areas has been compiled to provide information on many aspects for land use optimization, sustainable development and environmental protection. The mapping approach was based on data provided by conventional onland field works, marine remote sensing survey and aerial photo interpretation. These data sources were integrated into a GIS platform allowing reliable mapping solutions. The geological formations encountered were grouped into individual geotechnical units according to uniformity in lithological character, while the seabed sub-bottom structure was also obtained through several seafloor thematic map compilation. Shoreline variability and evolution for a long time period (1945–2008) were also investigated and mapped. The synergistic use of the results deduced from those disciplinary surveys is finally presented in a single engineering geological map covering the onshore and offshore area.

Keywords Engineering geological map · Marine remote sensing survey · Photogrammetry · Shoreline

Introduction

The coastline zone constitutes a dynamic part of seascape since its shape is affected by several natural factors (climate,

geology, hydrography, vegetation). Anthropogenetic activities have also a crucial contribution in modifying the existing dynamic equilibrium. A detailed coastal zone mapping including both the wider inland and seabed area is needed to understand the driving factors and to provide the accurate data for coastal resource management and sustainable development planning.

Traditional methods for coastal mapping are based on conventional field surveys and on aerial photo interpretation. Satellite remote sensing data has also been used and a large number of methods are available for mapping coastline from different sensors (Kevin and Asmar 1999; Frazier and Page 2000; Ryu et al., 2002; Guariglia et al., 2006). Marine remote sensing has become a common practice to study the submerged coastal landscapes especially in areas of great archaeological interest. Detailed surveys in submarine coastal sites using marine remote sensing techniques such as sidescan sonar and seismic profiling reveal evidence for human presence along ancient coastlines contributing further to the coastal landscape reconstruction. More recently, the mapping of submerged paleoshorelines resulting from high resolution geophysical methods has been led to the detailed paleogeographic reconstruction of submerged areas of great archaeological importance (Van Andel and Lianos 1984; Kraft and Rapp 1998; Wiedicke et al., 1999; Shennan et al., 2000; Papatheodorou et al., 2008; Chalari et al., 2009; Papatheodorou et al., 2014).

The aim of this paper is to present the synergy of multi disciplinary surveys such as marine remote sensing survey, aerial photogrammetry and in situ geological-geotechnical mapping, which have been carried out at Limeni Bay and the surrounding area, in order (i) to construct a single engineering geological map and (ii) to define the long-term and short-term coastal evolution. Totally different data sets of inland and offshore data are imported in a GIS geodatabase, collated, interpreted and finally presented in a simple

Communicated by: H. A. Babaie

✉ Konstantinos G. Nikolakopoulos
knikolakop@upatras.gr

¹ Department of Geology, University of Patras, University campus, 26504 Rio Patras, Greece

engineering geological map covering the onshore and offshore area. That engineering geological map presents the main geotechnical units of the onland area, the sediments thickness/bedrock head depth aerial distribution and the onshore/offshore structural framework of whole of the area. Moreover, that integrated survey recomposes the coastal evolution of the area, which is of great palaeoanthropological importance, over tens of thousands years (long-term) to tens of years (short-term) using marine remote sensing techniques and photogrammetry, respectively.

Geographical and geological setting of the area

Location

The site studied is located at the southern Peloponnese (Fig. 1) and is the southernmost inland area of continental Europe. Limeni Bay constitutes a natural safe harbor, since ancient time, on the West Coast of Mani Peninsula. Beautiful traditional villages are sited seaside (Limeni, N. Oitylo, Karavostasi), and around Oiitylo (Itylo) at 240 m a.s.l. and Areopolis at

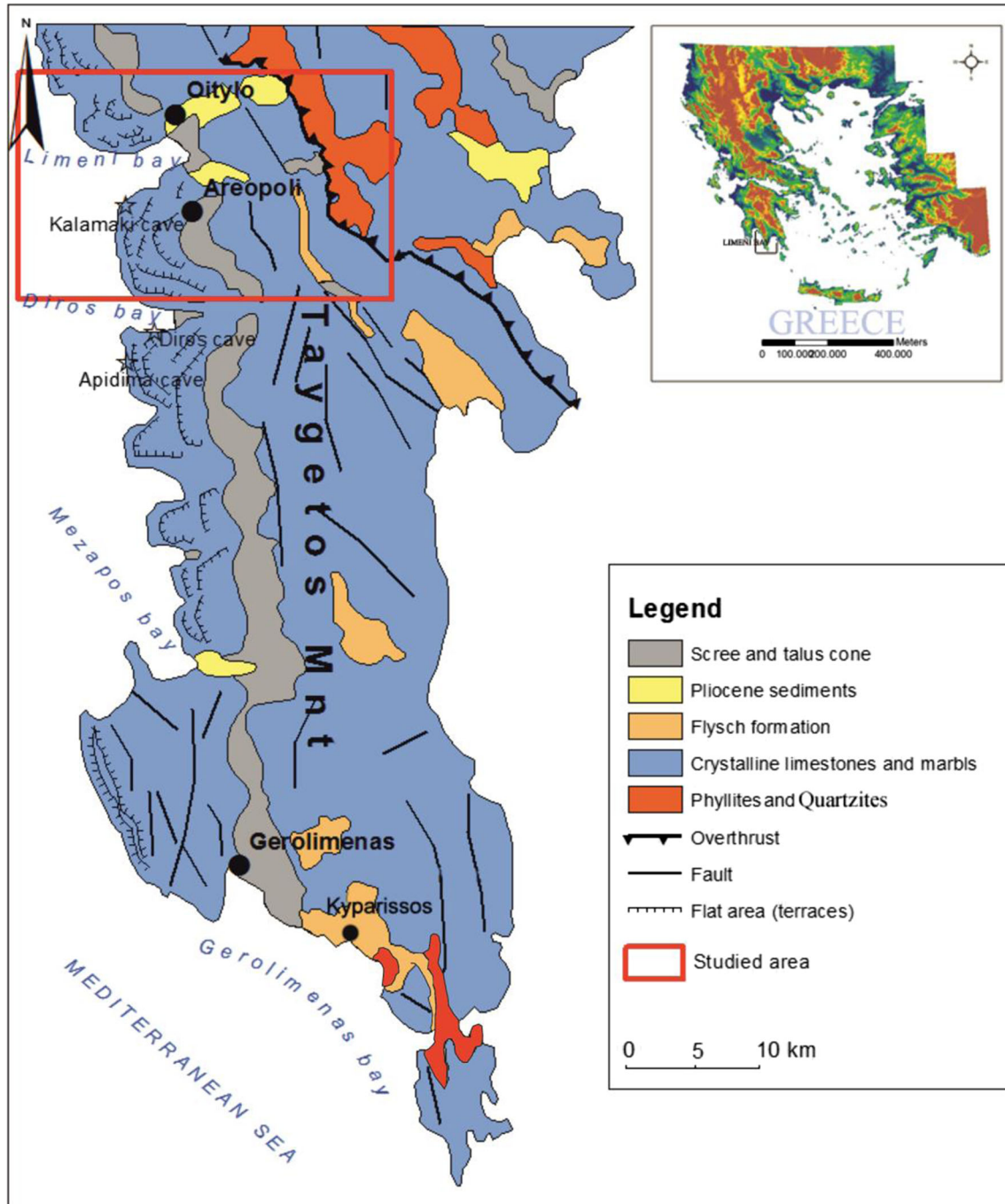


Fig. 1 Simplified geological map of Mani peninsula and location map of the studied area

250 m a.s.l. As tourism and population increase and settlements continue to expand, there has been increased pressure on the environment. Although the region is protected by EC environmental restrictions (NATURA 2000) man's activities have a harmful effect on the natural systems and the need to overcome problems that arise, or may arise in the future, require the establishment of rules for sustainable development.

Geological context and paleoanthropology

The autochthonous system of Plattenkalk unit which is tectonically overlaid by the Phyllite-Quartzite unit series constitutes the geological basement of Mani Peninsula. Both units display HP - LT metamorphism (Bassias and Triboulet, 1994; Doutsos et al. 2000; Micheuz et al., 2015). The Plattenkalk unit includes marble and schists of Upper Carboniferous to Upper Triassic, dolomitic marbles of Upper Triassic to Lower Jurassic, marbles and crystallized limestones with nodular cherts of Lower Jurassic to Eocene and flysh deposits of Middle Oligocene. The allochthonous Phyllite-Quartzite Unit is represented by phyllites, quartzites, metaconglomerates and marbles and corresponds to an Upper Carboniferous to Triassic rift sequence (Robertson, 2006; Chatzaras et al. 2006). Small extensional sub-basins were formed during the Plio-Pleistocene period where marls, sandstones and mudstones have accumulated (Zelilidis and Kontopoulos, 1999). The Quaternary deposits are mainly represented by talus cones and scree that in some cases have been acceded into the recent coastal sediments. These deposits often fill the caves located along the western coast including very important paleoanthropological remains. A simplified geological map is shown in Fig. 1.

Mani region generally presents a quite steep and highly relief controlled by fault fracture pattern, with steep slopes, well developed terraces along the western coasts and coastal cliffs formed in the limestones and marbles. The presence of extended tilted flat areas (terraces) demonstrates the non continuous uplift to the west and subsidence to the south. An uplift of more than 400 m has occurred during the Quaternary period in the north-western part of Mani Peninsula (Kelletat and Gassert 1975). In the southern part, some of these terraces have been found submerged under the sea indicating that earlier uplift has been followed by subsidence in the Late Quaternary. The differential vertical movements continue to affect the region. The ruins of ancient Kainipolis (growth at the 3rd century B.C.), located in southern Mani Peninsula near Kyparissos village, are observed 10 m below sea level.

The region is generally affected by many subvertical faults striking NNW-SSE and E-W, which have strongly contributed to the formation of the almost rectilinear shoreline and orthogonal or crescent shape bays. Extensional tectonics has dominated since the upper Miocene period resulting in the formation of sedimentary sub-basins and the followed deformation of their infillings. A number of sub parallel normal faults are

observed mainly between Gerolimenas and Mezapos bays (Fig. 1) presenting polished fault surfaces with tectonic striations in the contact of Mesozoic crystalline limestones with the Quaternary cemented scree (Rondoyanni et al., 1995).

The homogeneous sequence of thick-bedded Triassic to Eocene crystalline limestones and marbles that constitute the main horizon of Plattenkalk unit, is strongly affected by karstification phenomena resulting in the formation of many inland and submerged caves (more than 100 large and small ones) along the western steep coasts and the near shore zone. These caves are distributed within two district zones at an elevation of about 5–6 m and 16–18 m above sea level and have been created by the combined effect of tectonic uplift, fracturing, sea-level fluctuations, wave action, groundwater discharge and geochemical reactions.

The most spectacular cave is the Diros Cave (Glyfada and Alepotrypa caves) that is regarded as one of the most beautiful lake caves in the world with its underground river drainage system at sea level and having a 2.5 km long winding passage way that is the main route for sightseeing by boat. Since 1980 systematic paleoanthropological researches (Pitsios et al., 1994; Darlas 1995; Kormazopoulou-Kagalou et al., 1995; Harvati et al., 2013) have been focused on the caves and the surroundings, discovering by excavations in scree and talus cone material, significant localities of human habitation from the Middle-Upper Pleistocene. The results have brought to light human fossils of both pre-Neanderthals and Cro-Magnon (*Homo sapiens sapiens*), Paleolithic artifacts indicative of the hunting of the humans and cultural remains (lithic and bone industries, burials, items of personal ornament, traces of fire etc). The field research and excavation of material from a series of caves and especially the human specimens from Apidima and Kalamakia caves (Fig. 1) add to the growing evidence of a strong Neanderthal presence in the region during the Late Pleistocene and are of particular significance for the paleoanthropological history of Greece and the human evolution in Europe as well.

Methodology and results

The methodology used in this study covers a wide range of techniques and was mainly based on field observation and mapping and on both marine geophysical data and remote sensing data through aerial photographs for offshore and on-shore respectively. Extended field mapping was performed including the recognition of the geotectonic units and the collection of many samples. In the laboratory of Engineering geology a lot of tests on intact rock material was performed. Spatial information like the tectonic lines and the geological formation boundaries and non spatial information such as the laboratory results was extracted from the engineering geology survey.

The marine geophysical survey was conducted with a suitably modified 10 m long vessel, over an area of approximately 3.80 km² (Fig. 2). The survey was carried out using an acoustic system that included: a high frequency 3.5 kHz sub-bottom profiling system consisting of a Model 5430 A GeoPulse Transmitter, a Model 5210 A GeoPulse Receiver, signal recording system through Triton Elics acquisition software package and an O.R.E. Model 132B over-the-side four transducer array. Positioning data was obtained by a Trimble 4000 Differential Global Positioning system (DGPS) with an R.M.S. accuracy of 2 m and a Magellan NV 6500 GPS. The data were collected at a boat speed of about 4 knots.

The sub-bottom profiler system emits medium to high frequency acoustic pulses in the form of acoustic conical beams. The acoustic pulses, which penetrate under the seabed are reflected back by the underlying layers and recorded on a continuously running chart, thus providing a geological profile (seismic or acoustic profile) of the seafloor beneath the path over which the system is towed.

Twenty 3.5 kHz sub-bottom profiler tracklines were surveyed (Fig. 2). The tracklines were generally run perpendicular to the coastline having a spacing of 180 to 200 m, while

two lines run almost parallel to the coastline (Fig. 2). A time base of 1 ms pulse length was used. The penetration achieved was varying from almost zero in areas of outcropping to about 30 m in unconsolidated sediments.

The seismic data were recorded graphically and imported and georeferenced into ArcView environment for post processing. A detailed description of the data post-processing approaches has been presented previously (Chalari et al., 2009). The interpretation of the seismic profiles was based on the definitions of Damuth (1975).

The digital photogrammetry resulted to both raster and vector results. Analogue and digital airphotos at different scales were processed in Erdas Imagine software. Orthorectified airphotos from 1945 to 2008 with a spatial resolution of 1 m were created and stored (raster data). Using those airphotos as basemap the shoreline (vector data) was digitized at different dates.

The multifunctional technology of Geographic information Systems is used in order to collect, storage, manage, process, analyze and cartographically represent the above described complex geoscientific information. All data is stored and processed in spatial database specially designed for the demands of

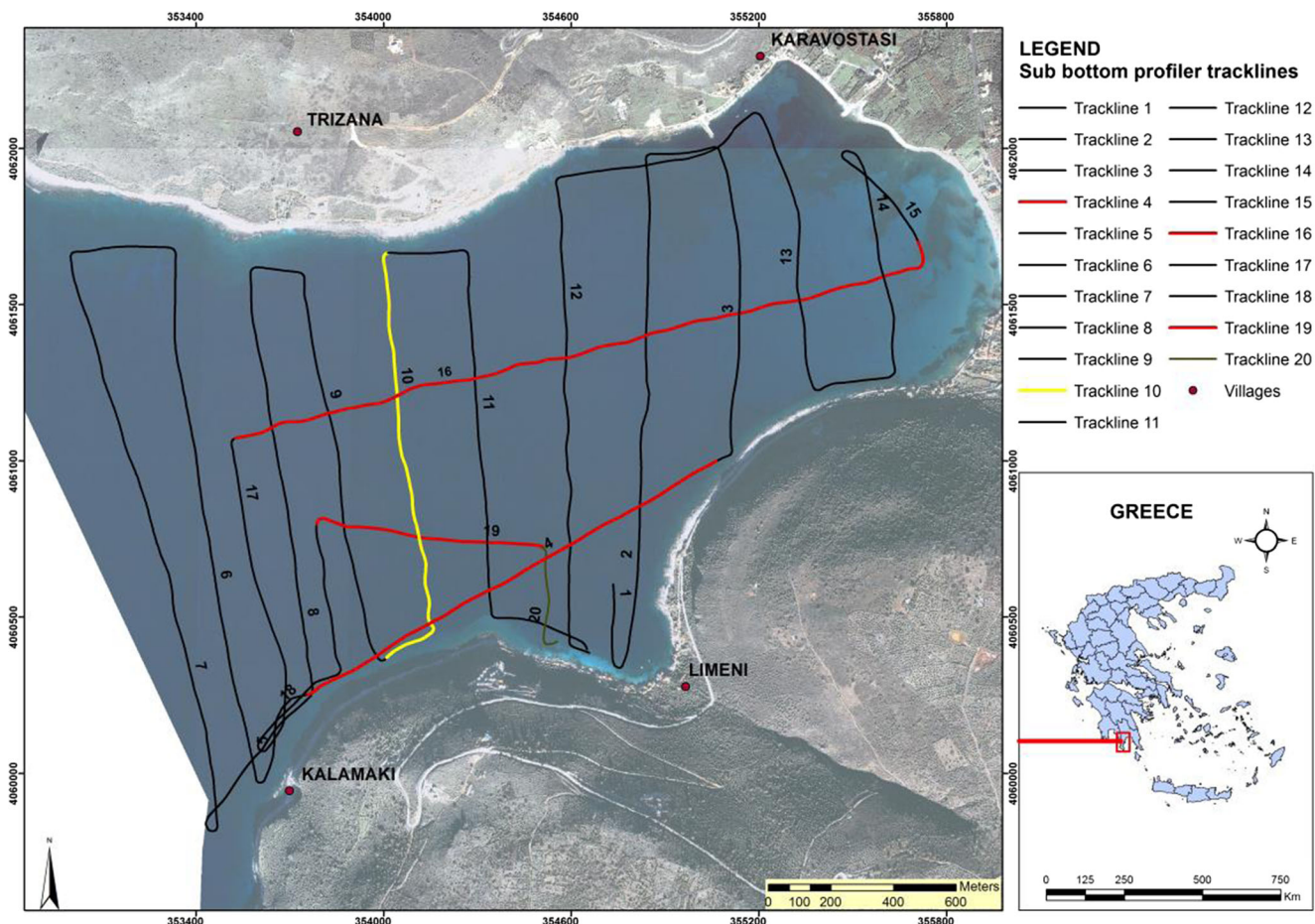


Fig. 2 Map showing the 3.5 kHz sub-bottom profiling tracklines. No 10 trackline (yellow color) corresponds to the seismic profile of Fig. 5. The footprint of tracklines 4, 19 and 16 (red color) appear also in Fig. 5

the specific project. The flowchart of the described methodology is presented in Fig. 3.

Ground conditions and engineering geological mapping

The engineering geological conditions of the region surrounding Limeni Bay were considered and a large scale engineering geological map was compiled at an original scale of 1:5000. In this map (Fig. 4), the geological formations encountered were grouped into seven (7) individual geotechnical units, based on the origin, relevant age, composition, physical state and engineering geological characteristics of the formations. Table 1 summarizes the results of the laboratory tests on intact rock material, including for each parameter the range of values, the mean value and the number of specimens tested. The total number of tested intact rock samples was one hundred and thirty five (135), while the stratigraphic horizons that they collected are also shown in Table 1. The parameters determined in dry conditions for a better comparison of the results, were as follows: total porosity (n_t), dry unit weight (γ_d), Schmidt Hammer Value (SHV), uniaxial compressive strength (σ_c), point loading index ($I_{s(50)}$), elastic Young’s modulus (E_t) and rock material constant, m_i obtained from the analysis of triaxial test data (Hoek and Brown 1997). The execution of laboratory tests was in accordance with ISRM suggested methods (ISRM 1981; ISRM 1985) and ASTM standards (ASTM 1986a; ASTM 1986b; ASTM 1993).

Unit 1: Mixed phases of recent deposits Brown, clayey sand (SC) and clayey, silty gravels (GM, GM-GC) constitute the main lithological types (about 80 %) of this Unit. *sandy*, stiff clay of low to medium plasticity (CL) and silt and sand (SM-SC, SM) are also encountered. These are loose deposits with a

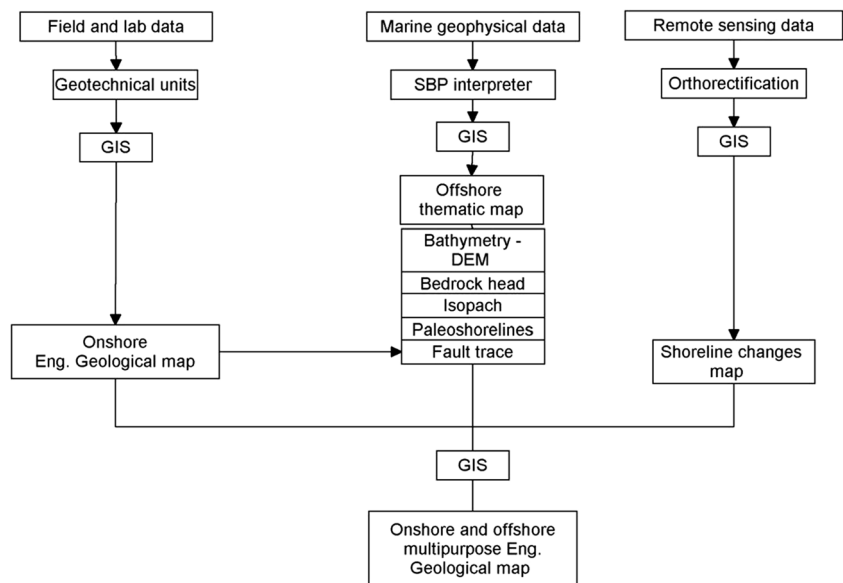
maximum thickness of about 5 m and they are permeable, with a phreatic level generally at the contact with the bedrock.

Unit 2: Talus cone and scree This unit consists of brownish-red, sandy-clayey materials of Upper (Wrm) to Middle (Riss) Pleistocene containing gravel pebbles and rock fragments. They are classified as clayey-silty gravels (GC, GM, GC-GM) and clayey sands (SC, SC-SM). The formation is well to medium cemented with clayey-marly matrix to breccia and fills the caves located along the western coast including important paleoanthropological findings.

Unit 3: Marly formations These are Plio-Pleistocene sediments mainly consisting of marls, calcareous sandstones and marly limestones that classified as poorly-washed biosparites (Folk 1962) while moderately to well cemented conglomerates are also encountered at the upper part of the unit. They have a maximum thickness of about 250 m and occupy the east-northeast-oriented area of Oitylo sub-basin. The marls are whitish-yellow, very stiff to hard, silty of low plasticity (CL-ML) with normal activity and constitute the lower horizon of the sequence. The calcareous sandstones and marly limestones are whitish-yellow to brownish-yellow, weak to medium strong with a characteristic porous and cellular structure.

Unit 4: Semi-metamorphosed flysch The unit consists of green-grey-colored, medium-thickly bedded, strong, slightly to moderately weathered and partly discolored metasandstones, intersecting by three main discontinuity sets with rough planar surfaces. The rockmass Geological Strength Index (GSI) values (Hoek and Brown 1997) range often from 45 to 55. Locally, highly weathered and decomposed clayey schist are also encountered.

Fig. 3 Flowchart of the approach applied for mapping purposes from the different data sources



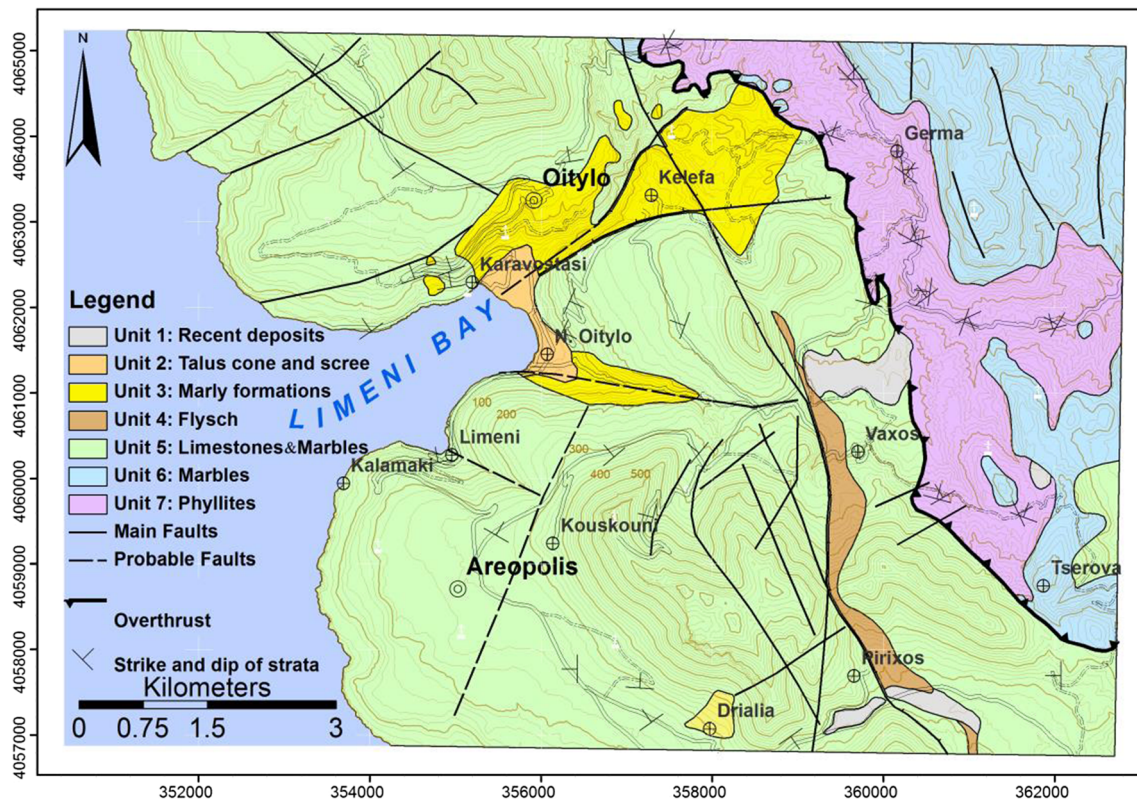


Fig. 4 Engineering geological map of Limeni bay wider area

Unit 5: Limestones and marbles These formations are Lower Jurassic to Eocene in age, grey, strong of medium hardness, compact, medium to thickly bedded, locally faulted, karstified, clastic and frequently brecciated, while they are classified as unsorted biosparites. The rockmass Geological Strength Index (GSI) values often range from 50 to 60.

Unit 6: Marbles The formation constitutes an horizon of Upper Triassic to Lower Jurassic in age. The marbles are grey to whitish-grey, strong to very strong of medium hardness, compact, medium to thickly bedded, while the rockmass Geological Strength Index (GSI) values often range from 55 to 65.

Table 1 Laboratory testing results on the intact rock material of geotechnical units

Rock material stratigraphic horizon		γ_d (kN/m ³)	n_t (%)	$I_{S(50)}$ (MPa)	SHV	σ_c (MPa)	E_t (GPa)	m_i
Unit 3: Marly limestone –	Range	17.2–19.1	21–29	0.5–1.5	38–40	12–31		
	Mean	18.4	25	1.23	39	24		
No of samples:16	no of tests	16	16	8	16	12		
Unit 4: Meta – sandstone	Range	23.8–26.8	<0.05	4.6–5.2	45–52	54–71	1.9–3.6	21–23
	Mean	25.7		4.8	49	63	2.7	
No of samples:32	no of tests	22	22	22	12	12	10	4
Unit 5: Crystalline Limestone	Range	26.3–26.7	0.3–0.5	3.5–5.6	53–50	68–82	3.4–7.2	6–7
	Mean	26.5	0.4	4.6	51	79	5	
No of samples:35	no of tests	25	25	18	22	15	7	4
Unit 6: Marble	Range	26.1–27.2	0.1–0.2	4.9–5.7	54–51	89–107	2.8–4.2	8–9
	Mean	26.8	0.2	5.4	52	98	3.7	
No of samples:34	no of tests	24	24	19	22	14	8	4
Unit 7: Phyllites	Range	25.3–26.7	0.5–2.2	1.6–4.7	43–48	20–79		
	Mean	26.1	1.7	2.8	45	49		
No of samples:18	no of tests	18	18	15	18	18		

Symbols as described in text

Unit 7: Phyllites The unit consists of grayish-black, brownish-gray, medium strong phyllites mica schists, blue-schists and quartzites moderately to highly weathered and locally completely decomposed and disintegrated. The great scatter of intact rock strength values shown in Table 1 is mainly due to the high anisotropy of the specimens tested and to the great dependence of loading direction to the schistosity planes (strength anisotropy).

Subbottom profiling and seafloor mapping

The examination of the acoustic profiles has shown that, the seabed on the records is characterized by three different Echo Types (Damuth, 1975), each one corresponding to different stratigraphy and seabed material. The first echo type is characterized by a prolonged surface reflector without any evidence of a deeper signal penetration and thus has no sub-bottom reflections. This type represents a rocky seafloor that appears in steep slopes and extends from the present day shoreline to a depth of about 20 to 30 m. The second echo type is characterized by an acoustically transparent unit locally with very weak internal reflectors that overlies a very prolonged reflector. This type represents unstratified sediments overlying the bedrock and its distribution is limited at the shallower part of the Limeni bay. The third echo type presents sharp to indistinct parallel, subparallel and locally divergent seismic reflections overlying a prolonged general flat reflector. It is located at the central and deeper part of the Limeni bay. This type is attributed to quite stratified sedimentary sequence which overlies the bedrock and thickens seawards, following the structurally-controlled seafloor morphology and reaching a maximum thickness of about 30 m (Fig. 5). The layered character of this sequence suggests that the sediments were deposited continuously and slowly (hemipelagic sedimentation). The divergent character of the seismic reflections against south-dipping fault indicates syn-tectonic deposit (Fig. 5).

The evaluation of seismic data collected along the dense grid of track lines using the Sub Bottom Profiler (SBP) Interpreter software and processed with Geographical Information System, led to the compilation of a series of seafloor thematic maps:

- The bathymetric map (Fig. 6) shows the water depth of the seafloor at 2 m intervals. The seafloor dip is increased southwest reaching a maximum depth of 190 m. As shown from both the contouring and the digital elevation model (DEM), the offshore slopes are steep near the shoreline (Figs. 6 and 7).
- The engineering geological map shows the depth of the bedrock head (Fig. 8) below the seafloor with contours at 2 m intervals. This map was compiled by digitizing the bedrock formation (surface and subsurface) on the sub-bottom profiling data. The bedrock depth data were processed in GIS environment.
- The isopach map of unconsolidated sediments (Fig. 9) provides contours showing the thickness of the unstratified and stratified sediments at 2 m intervals. Those sedimentary units probably are consisted of loose sandy – silty sediments of low strength. Their thickness is up to 32 m.
- Detailed examination of the profiles on the bedrock surface reveals the presence of small scarps which appear as sharp breaks in the overall slope gradient of the limestone surface (Fig. 5). These scarps on the bedrock appear to have been sculptured by the erosional power of the waves when the sea level was at a standstill for a short period of time during the sea transgression. It can therefore be considered as evidence of palaeoshoreline. The water depth of each submerged palaeoshoreline has been also measured (Fig. 10). The age of those submerged palaeoshorelines can be estimated using local sea-level change curve and thus the palaeoshoreline distribution map greatly enhance the understanding of the palaeogeographic evolution of the area

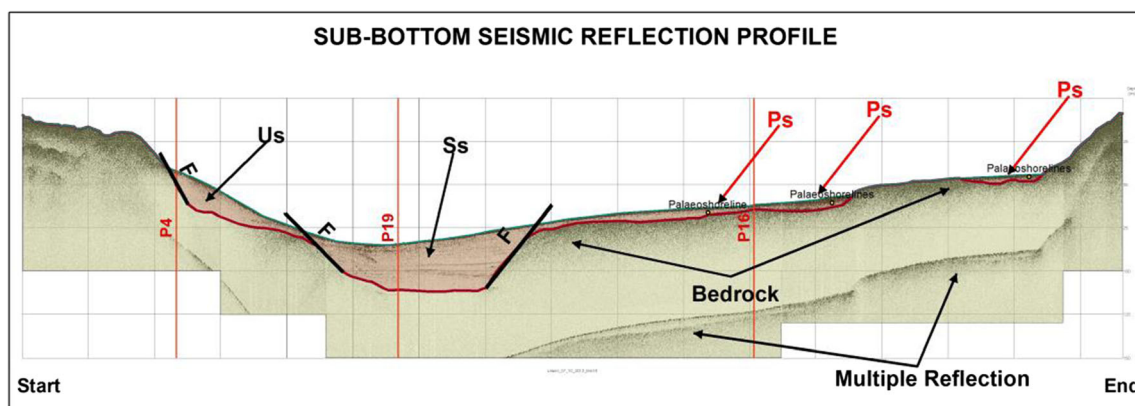
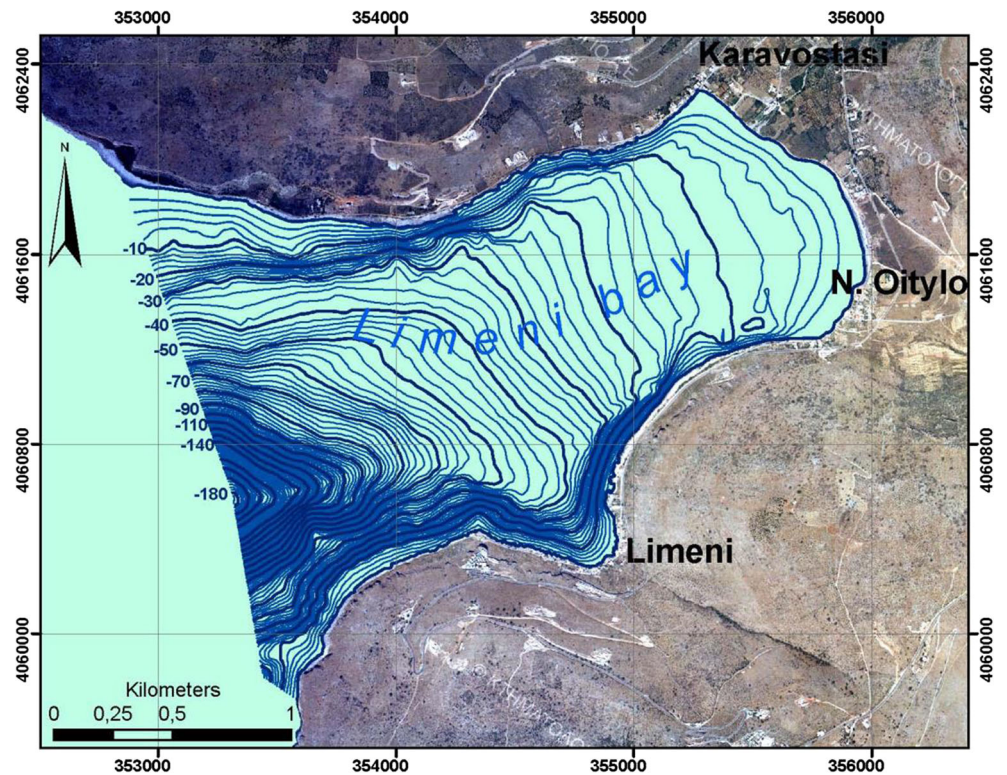


Fig. 5 Representative sub-bottom seismic reflection profile along the No 10 trackline showing the bedrock, the unstratified (Us) and stratified (Ss) sediments, the fault traces (F) and the surface or buried submerged

palaeoshorelines (Ps). The footprints of the tracklines no 4, 19 and 16 can be observed in red color

Fig. 6 Bathymetric map based on the sub-bottom profiling data. The background is an orthophoto of the Greek Cadastral with 25 cm spatial resolution



which is of great importance from palaeoanthropological point of view.

- The offshore fault map of the Limeni bay was based on the detected faults exclusively on high resolution 3.5 kHz subbottom profiles (Fig. 11). Faulting was recognized in the seismic profiles on the basis of significant changes in reflection continuation and acoustic character. Correlation

of faults between survey tracklines has been made on the basis of seismic reflection deformation style, relative vertical displacements and the bathymetric morphology. Faulting in Limeni bay is characterized by the abrupt termination of seismic reflections of the third echo type against the bedrock (Fig. 11). In some cases, the seismic reflections exhibit a concave-upward geometry indicating

Fig. 7 Digital Surface Map of seabed. The depth ranges from 0 to -192 m. The background is an orthophoto of the Greek Cadastral with 25 cm spatial resolution

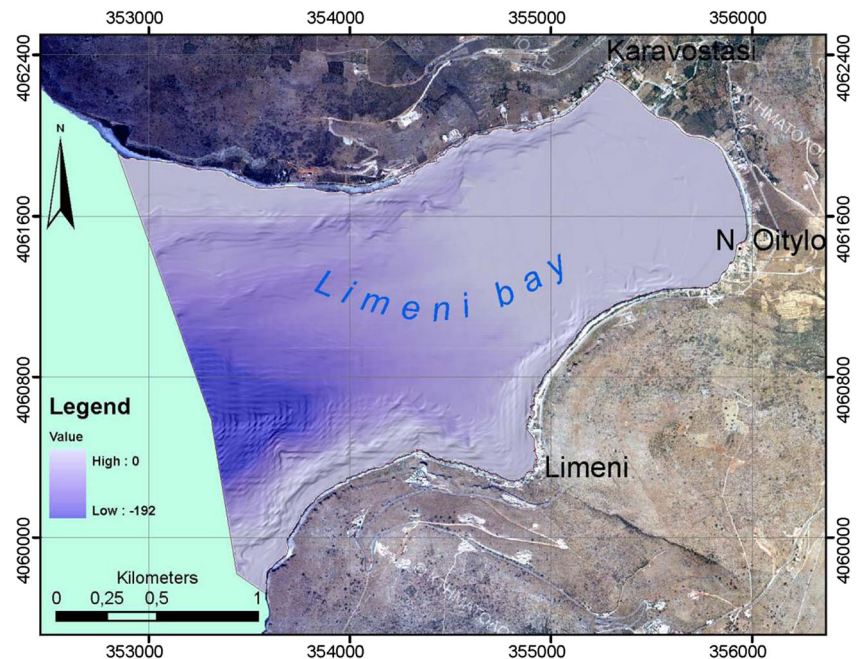
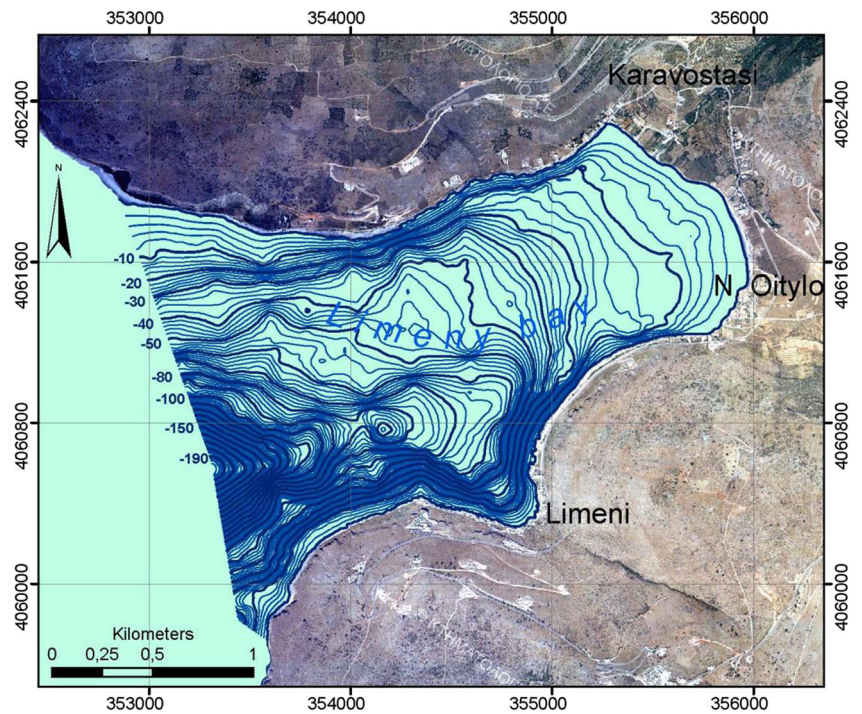


Fig. 8 Contour map showing the depth of the bedrock head below the seafloor. The background is an orthophoto of the Greek Cadastral with 25 cm spatial resolution



a normal drag. Syndepositional faulting has been also detected by progressive increases of the sedimentary unit thickness on the down-thrown side of the south-dipping fault (Fig. 11). Moreover, faulting does not produce seabed displacements indicating that the faults in the Limeni bay became progressively buried by the recent sediment cover (Fig. 11). It should be noted that the offshore faults in the Limeni bay

have been obtained using a high resolution profiler with maximum penetration of about 30 m. In order to study, in detail, fault geometry at depth, another type of sub-bottom profiler is needed. A profiler producing pulses of higher energy and lower frequencies and allowing greater penetration with lower resolution could achieve better records of the fault continuation to greater depths below the seabed.

Fig. 9 Isopach map of the unconsolidated sediments. The background is an orthophoto of the Greek Cadastral with 25 cm spatial resolution

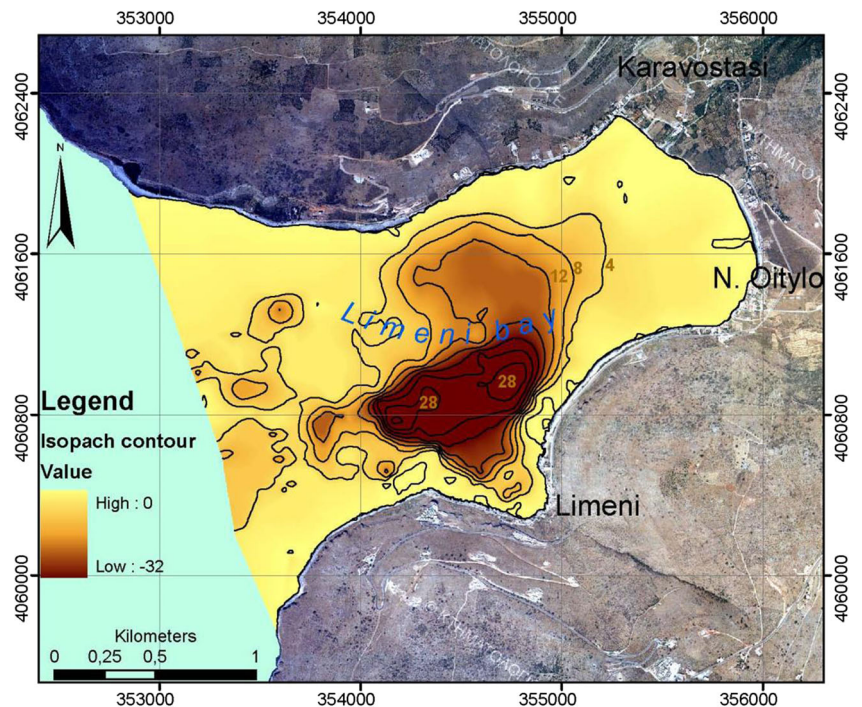
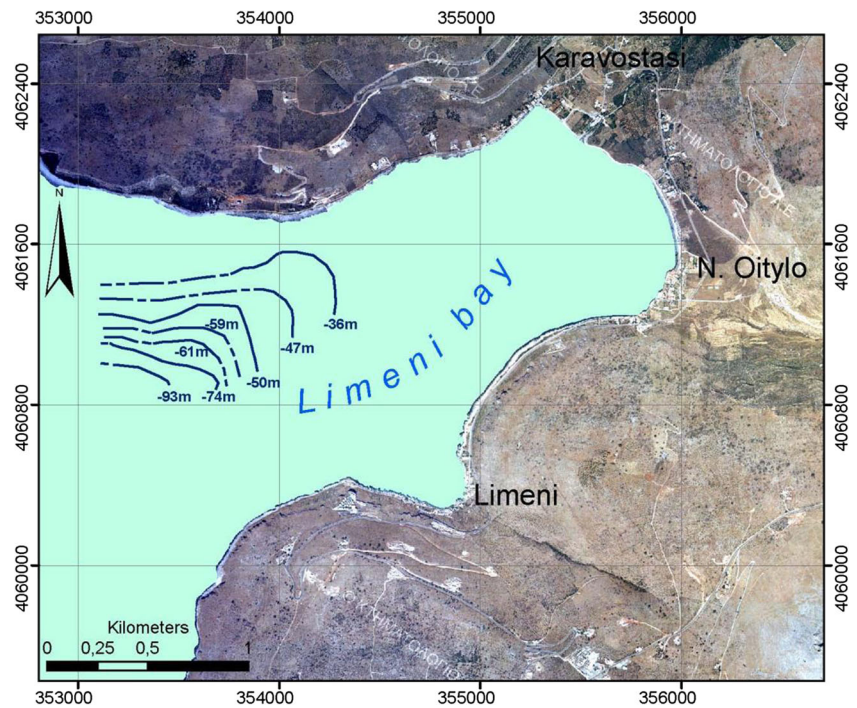


Fig. 10 Map showing the submerged paleoshorelines. The water depth in which the submerged palaeoshorelines have been detected is also mentioned on the map. The background is an orthophoto of the Greek Cadastral with 25 cm spatial resolution

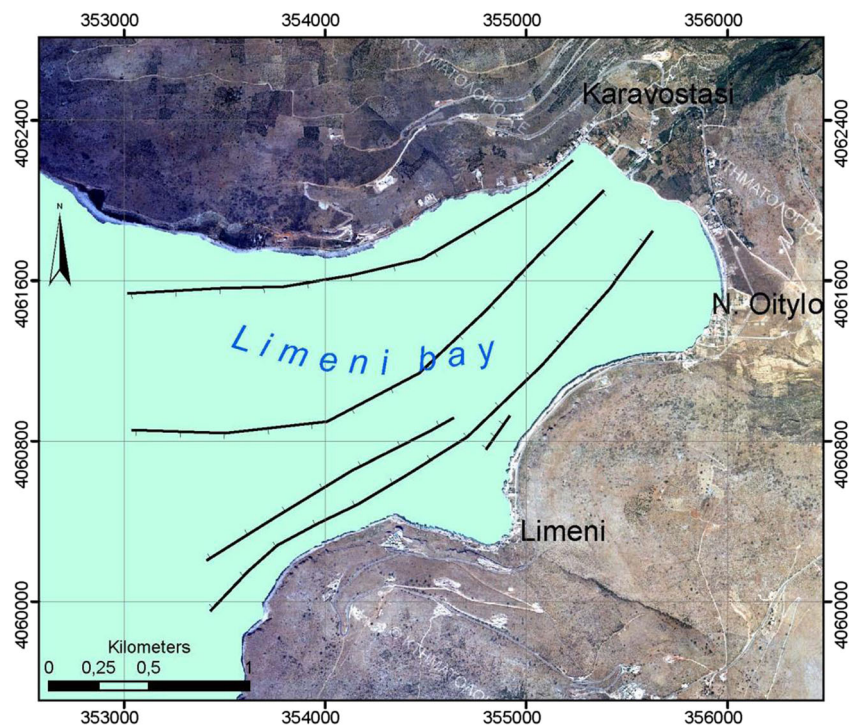


- A synthesis of the unconsolidated sediments data together with the offshore faulting, by superimposing the maps of Figs. 9 and 11, showed that the tectonic axis of the small graben system coincides well with the depocentre of maximum sediment thickness of about 30 m. Moreover, the depocentre also coincides well with a small basin that has been formed in the bedrock (Fig. 8).

Aerial photogrammetry and shoreline changes mapping

Shoreline changes that include the results of long term erosion or accretion and short-term impacts of severe storms were investigated remotely using aerial photographs. The study was focused on coastal erosion rates and patterns along the entire sandy – pebbly shoreline of Limeni Bay. Both analog

Fig. 11 Map showing the offshore faults at the Limeni bay. The background is an orthophoto of the Greek Cadastral with 25 cm spatial resolution



and digital air-photos were used to analyze the coastline evolution over the time period from 1945 to 2012. Classical analog airphotos covered the period from 1945 to 1989, digital airphotos for 2008 and recent Google Earth images were used. The air photos of the years 1945, 1960 and 1989 have been orthorectified with the Leica Photogrammetry Suite, while ground control points and a high accuracy DSM were also used.

The 2008 digital air photo mosaic with a spatial resolution of 0.25 m was obtained from the Hellenic Cadastral (Ktimatologio S.A.) and the respective DSM was used as the base map for all the other data sets. The RMS error was less than 0.004 pixels. Tides were not taken into account for the estimation of the shoreline evolution since they are very low in the Mediterranean Sea.

The validity of orthorectification process was verified using characteristic ground features (e.g. historical ruins) identified in all the available photo series. From the digital airphoto of the Greek Cadastral four (4) characteristic features (old house, road, historic castle and stone fence), that can be recognized in all the analogue airphotos from 1945 to 1989, were digitized (Fig. 12). As shown in Fig. 12 those features were accurately matched in all the orthorectified airphotos.

The shorelines of different airphoto mosaics were digitized and projected using GIS software tool and the evolution of the

shore was estimated for the period 1945–2008 as shown in Fig. 13. Based on the estimation of shoreline change rate, the shoreline has been retreated inland, due to erosion, about 0.25 to 0.40 m per year for northern (Karavostasi village) and southern part of the beach (N. Oitylo village) respectively. The shoreline retreat is primary attributed to the lack of sediment supply and wave-driven erosion which are exacerbated by the eustatic sea level rise. Small scale human activities (e.g. small piers) have increased the rate of shoreline retreat. The slightly lower rate of shoreline retreat of the northern part of the beach compared to the southern part, is probably attributed to the limited sediment supply by a ephemeral stream which flows close to Karavostasi village.

Multiple use map

The final result of the combined use of engineering geology, marine geophysics, and photogrammetry was the compilation of the single map of Fig. 14 that provides a generalized representation of all those significant components of inland and offshore geological environment. For engineering and environmental purposes the types of map that may be prepared are many and varied. It is desirable to categorize them in some way, as for example has initially proposed in several guidebooks [IAEG 1976; Dearman 1991) by the criteria of purpose,

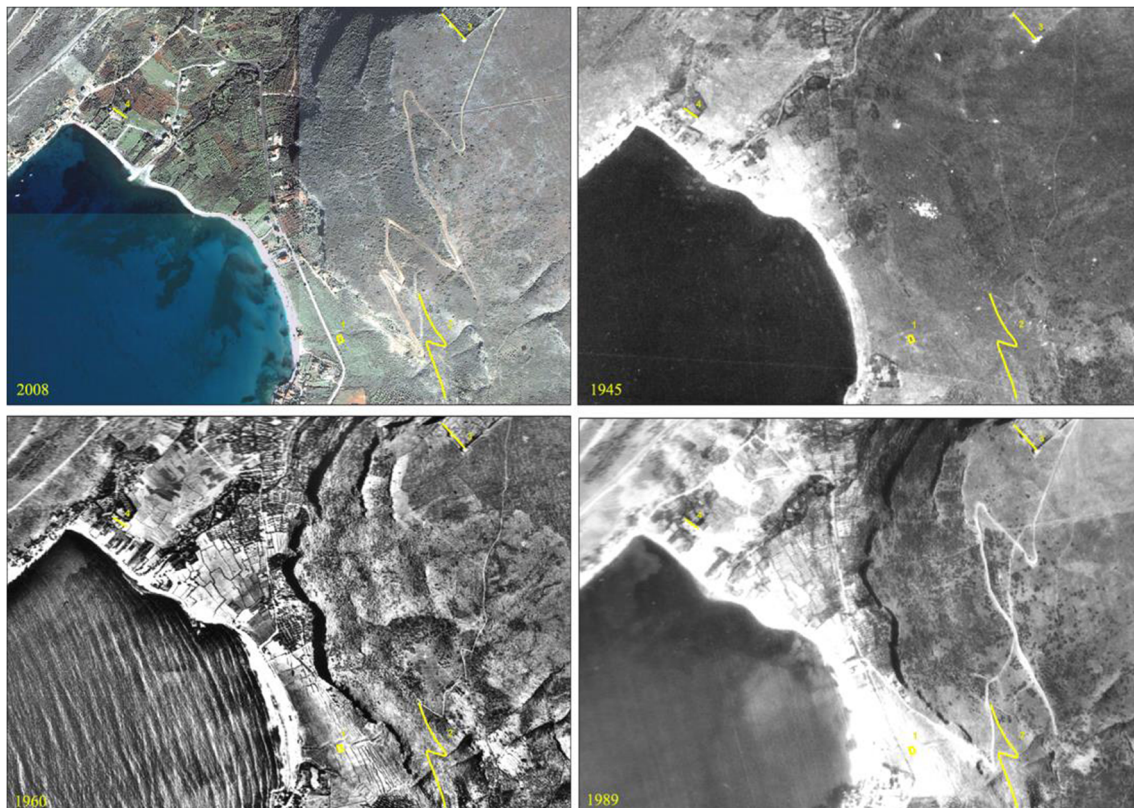
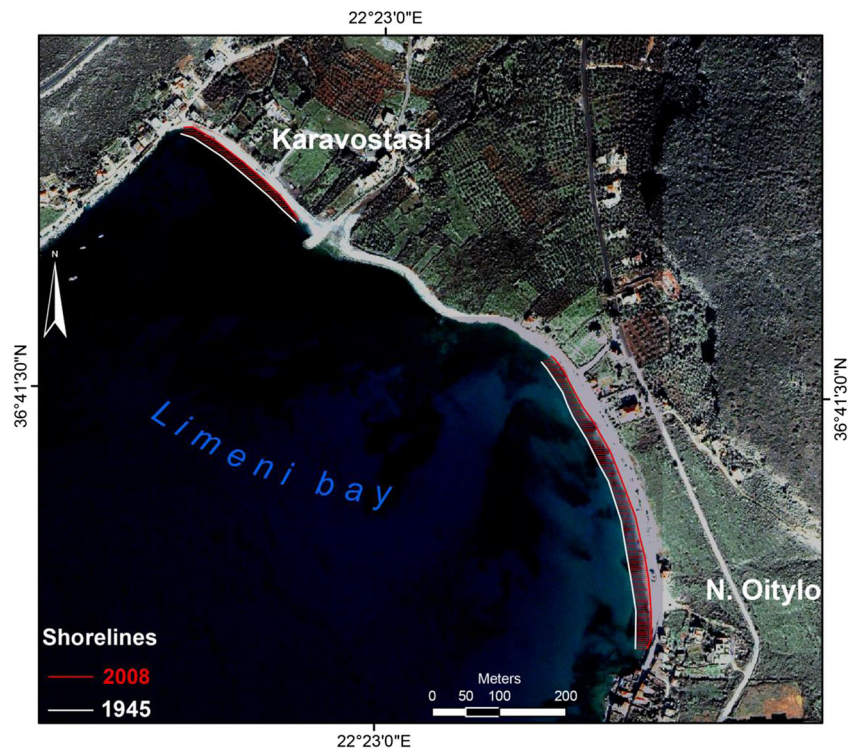


Fig. 12 The digital airphoto mosaic of the study area, provided by the Greek Cadastral with a spatial resolution of 25 cm and the orthorectified airphotos of 1945, 1960 and 1989. The four yellow-colored characteristic

features that were digitized in order to control the orthorectification accuracy are also shown in all the photos

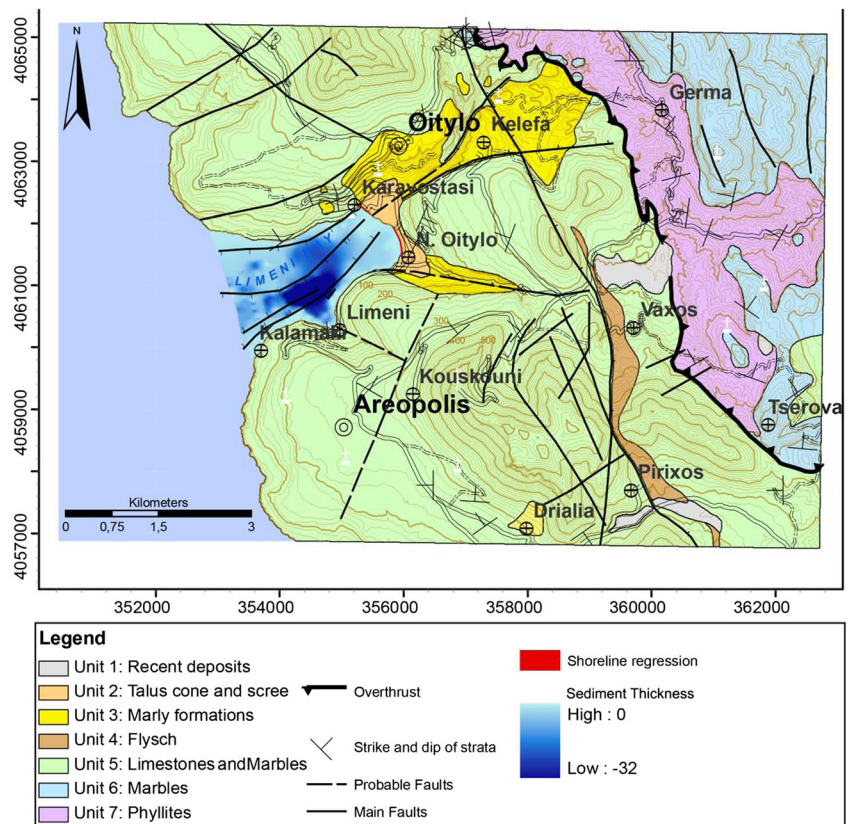
Fig. 13 The estimated shoreline changes for the period of 1945 to 2008



content and scale. Comprehensive maps, as the name imply, attempt to show everything of relevance in the engineering geological environment while multi-purpose (or general-

purpose) are intended to provide information on the many aspects of engineering geology for various planning and engineering purposes. So the finally compiled map constitutes a

Fig. 14 Onshore and offshore engineering geological map of the Limeni bay wider area



medium scale comprehensive multipurpose engineering geological map including both onshore and offshore areas.

Discussion and conclusions

Through this integrated study several techniques for obtaining data and “mapping” this data to be suitable for the needs of civil engineering, environmental assessments and palaeogeographic reconstruction are developed, including both inland and offshore environment.

Much work is being done using marine remote sensing methods in order to obtain an accurate picture of the seafloor conditions. Seabed engineering geological conditions have shown that long-term complex geologic processes govern the large-scale evolution of the coastal landscape of the area. The paleogeography of the coastal settings can be reconstructed and related to archaeological settings and historical incidents.

A reliable short-term (1945–2008) shoreline evaluation is also obtained using aerial photogrammetry. Understanding the nature of past changes in the coastal landscape and combined that with the study of present human alterations can be used for better prediction and projection of the future long- and short-term natural and/or human induced changes at the coastal zone.

From a technical viewpoint, the main outcome of this work consists in the setting up of reliable solutions for engineering geological mapping including both onshore and offshore areas in a quantitative framework, using multi source data through the development and implementation of a GIS-based experimentation and demonstration platform.

Acknowledgments Special thanks go to Dr. D. Christodoulou for his great support during the marine remote sensing survey.

References

- ASTM (1986a) Standard test method of unconfined compressive strength of intact rock core specimens. ASTM Stand 04.08(D2938)
- ASTM (1986b) Standard test method for triaxial compressive strength of undrained rock core specimens without pore pressure measurement. ASTM Stand 04.08(D2664)
- ASTM (1993) Standard test method for elastic moduli of intact rock core specimens in uniaxial compression. ASTM Stand. 04.08(D3148)
- Bassias Y, Triboulet C (1994) Tectono-metamorphic evolution of blueschist formations in the Peloponnesus (parnon and taygetos massifs, Greece) - a model of nappe stacking during tertiary orogenesis. *The Journal of Geology* 102(6):697–708
- Chalari A, Papatheodorou G, Geraga M, Cristodoulou D, Ferentinos GA (2009) Marine geophysical survey illustrates Alexandria's Hellenistic past. *Z. Geomorph. N.F., Berlin-Stuttgart*, 53, Suppl 1, 191–212, doi:10.1127/0372-8854/2009/0053S1-0191.
- Chatzaras V, Xypolias P and Doutsos T (2006) Exhumation of high-pressure rocks under continuous compression: a working hypothesis for the southern Hellenides (central Crete, Greece). *Geol Mag*, 143, 859–876. <http://dx.doi.org/10.1017/S0016756806002585>.
- Damuth J (1975) Echo character of the western equatorial Atlantic floor and its relationships to the dispersal and distribution of terrigenous sediments. *Mar Geol* 18:17–45
- Darlas A (1995) L'industrie lithique trouvee avec le squelette de femme LAO 1/S3 de la grotte d'apidima (Mani-Greece). *Acta Anthropologica* 1:59–64
- Dearman W (1991) Engineering geological mapping. Butterworth – Heinemann Ltd.
- Doutsos T, Koukouvelas I, Poulimenos G, Kokkalas S, Xypolias P, Skourlis K (2000) An exhumation model of the south Peloponnesus, Greece. *Int J Earth Sci* 89(2):350–365. doi:10.1007/s005310000087
- Folk R (1962) Spectral subdivision of limestone types. In: Ham WE (ed) *Classification of Carbonate Rocks*, AAPG Memoir No. 1, Tulsa, pp. 62–84
- Frazier PS, Page KJ (2000) Water body detection and delineation with Landsat TM data. *Photogramm Eng Remote Sens* 66(2):1461–1467
- Guariglia A., Buonamassa A., Losurdo A., Saladino R., Trivigno M., Zaccagnino A. (2006) A multisource approach for coastline mapping and identification of shoreline changes. *Ann Geophys.*, vol. 49, N.1, 295–304.
- Harvati K, Darlas A, Bailey S, Rein T, El Zaatari S, Fiorenza L, et al. (2013) New Neanderthal remains from Mani peninsula, southern Greece: the kalamakia middle Paleolithic cave site. *J Hum Evol* 64(6):486–499
- Hoek E, Brown ET (1997) Practical estimates of rock mass strength. *Int J Rock Mech Min Sci Geomech Abstr* 34(8):1165–1186
- IAEG (1976) Commission on Eng. Geological Maps, Engineering geological maps. A guide to their preparation. The Unesco Press, Paris.
- ISRM (1981) Suggested Methods, Rock Characterization Testing and Monitoring. Pergamon Press, Oxford., 113–116 and 123–127.
- ISRM (1985) Suggested methods, suggested method for determining point-load strength. *Int. J. Rock mech. Min. Sci. Geomech Abstr* 22:53–60
- Kellettat D, Gassert D (1975) Quartargeologische untersuchngen im kustenraum der mani-halbinsel, peloponnes. *Z Geomorphol* 22:8–56
- Kevin W, El Asmar HM (1999) Monitoring changing position of coastlines using thematic mapper imagery, an example from the Nile delta. *Geomorphology* 29:93–105
- Kormazopoulou-Kagalou L, Protonotariou-Deilaki E, Pitsios P (1995) Paleolithic skull burials at the cave site of apidima. *Acta Anthropologica* 1:119–125
- Kraft J, Rapp J (1998) Geological reconstruction of ancient coastal landforms in Greece with predictions of future coastal changes. In: marinos P, koukis G., (Eds.) *the engineering geology of ancient works, monuments and historical sites preservation and protection*. Balkema, Rotterdam, vol 3:1545–1556
- Micheuz, P., Krenn, K., Fritz, H., Kurz, W. (2015). Tectonometamorphic evolution of blueschist-facies rocks in the Phyllite-Quartzite Unit of the External Hellenides (Mani, Greece). *Austrian J Earth Sci*, 108/1, 109–122, doi:10.17738/ajes.2015.0007.
- Papatheodorou G, Geraga M, Ferentinos G (2008) The reconstruction of prehistoric shorelines in Dokos island, AegeanSea, using remote sensing techniques. In: Y. F. N. Z, K. P (eds) *Proceedings of the 4th Symposium of the Hellenic Society for Archaeometry*, pp. 65–71
- Papatheodorou G, Geraga M, Christodoulou D, Iatrou M, Fakiris E, Heath S, Baika K (2014) A geoarchaeological survey, cape sounion, Greece: preliminary results. *Mediterranean Archaeology and Archaeometry* 14(1):357–371
- Pitsios T., Mettos A., Rondoyanni T., Georgiou C., (1994) Paleoanthropological research in the region of Areopolis, Laconia. In: *Hell. Speleol. Soc. Bull. (Ed.)*, 5th Intern. Congress of Hellenic

- Sperological Society Cave Development, Evolution and Environment, Athens 208 (in Greek)
- Robertson A (2006) Sedimentary evidence from the south Mediterranean region (Sicily, Crete, Peloponnese, evia) used to test alternative models for the regional tectonic setting of Tethys during late palaeozoic-early Mesozoic time. In: A.H.F. Robertson, and D. Mountrakis (eds.), tectonic development of the eastern Mediterranean region. *Geol Soc Lond Spec Publ* 260:91–154
- Rondoyanni T, Mettos A, Georgiou C (1995) Geological and morphological observations in the greater oitilo-diros area, Mani. *Acta Anthropologica* 1:93–102
- Ryu JH, Won JS, Duck Min K (2002) Waterline extraction from Landsat TM data in a tidal flat. A case study in gomso bay, Korea. *Remote Sens Environ* 83:442–456
- Shennan I, Lambeck K, Flather R, Horton B, McArthur J, Innes J, et al. (2000) Modeling western north sea palaeogeographies and tidal changes during the Holocene. In: Shennan I, Andrews J (eds) Holocene land – ocean interaction and environmental change around the north sea, Geological Society. *Spec. Publ*, London, pp. 299–319
- Van Andel TH, Lianos N (1984) High resolution seismic reflection profiles for the reconstruction of post-glacial transgressive shorelines: an example from Greece. *Quat Res* 22:31–45
- Wiedicke M, Kudrass HR, Hubscher C (1999) Oolitic beach barriers of the last glacial sea level lowstand at the outer Bengal shelf. *Mar Geol* 157:7–18
- Zelilidis A, Kontopoulos N (1999) Plio-pleistocene alluvial architecture in marginal extensional narrow sub-basins: examples from south-west Greece. *Geol Mag* 136(3):241–262